A NEUTRINO INTERACTION SIMULATION PROGRAM LIBRARY NEUT*

Yoshinari Hayato

Kamioka Observatory, ICRR, University of Tokyo
Higashi-Mozumi 456, Kamioka-cho, Hida-city Gifu 506-1205, Japan

(Received July 2, 2009)

A neutrino interaction simulation program library NEUT has been developed for the studies of the atmospheric neutrino and the accelerator neutrinos. In this article, the models and the implementations of neutrino interactions in NEUT are described. Also, the nuclear effects of generated particles are discussed.

PACS numbers: 13.15.+g, 14.60.Lm, 23.40.Bw, 24.10.Lx

1. Introduction

NEUT is a program library to simulate neutrino interactions with nucleon and nucleus. This program library was initially developed to study the interactions of atmospheric neutrino and to estimate the detection efficiencies of nucleon decay with the water Cherenkov detector, Kamiokande [1]. Since then, NEUT has been continuously updated and used in the various experiments like Super-Kamiokande, K2K, SciBooNE and T2K. As described, one of the main application of NEUT is to simulate the interactions of atmospheric neutrino in the water Cherenkov detector. Therefore, this program library covers a wide energy range of neutrino from several tens of MeV to hundreds of TeV. The primary target material of neutrino interaction are hydrogen and oxygen, which are constituents of water. However, the recent neutrino detectors use also the scintillator or iron as the interaction target material. Therefore, the program library has been updated to simulate neutrino interactions with various nuclei including carbon, argon and iron.

In the following sections, neutrino interaction models and their implementations including the interactions of generated particles in the nuclei are described.

* Presented at the 45th Winter School in Theoretical Physics "Neutrino Interactions: From Theory to Monte Carlo Simulations", Lądek-Zdrój, Poland, February 2–11, 2009.

2. Neutrino interactions

In NEUT, following neutrino interactions are considered:

Charged/neutral current (quasi-)elastic scattering
$(\nu\, N \rightarrow l\, N')$,
Charged/neutral current single π production
$(\nu\, N \rightarrow l\, N'\, \pi)$,
Charged/neutral current single γ production
$(\nu\, N \rightarrow l\, N'\, \gamma)$,
Charged/neutral current single K production
$(\nu\, N \rightarrow l\, \Lambda\, K)$,
Charged/neutral current single η production
$(\nu\, N \rightarrow l\, N'\, \eta)$,
Charged/neutral current deep inelastic scattering
$(\nu\, N \rightarrow l\, N'\, \mathrm{hadrons})$,
Charged/neutral current coherent π production
$(\nu\, ^{16}\mathrm{O} \rightarrow l\, \pi\, X)$,

where N and N' are the nucleons (proton or neutron), l is the lepton, and X is the remaining nucleus, respectively.

2.1. Elastic and quasi-elastic scattering

The cross-section for the neutrino nucleon charged current quasi-elastic scattering is evaluated based on the model of Llewellyn-Smith [2]. In order to obtain the cross-section off nucleons in the nucleus, it is necessary to take into account the in-medium effects. In NEUT, the relativistic Fermi gas model by Smith and Moniz [3] is used to calculate the cross-section off nucleons in the nucleus. Both models use the vector and the axial-vector form factors of nucleon. Those form factors are assumed to be dipole in the original articles. On the other hand, the vector form factor is measured by the recent precise electron scattering experiments and known to have some deviation from the simple dipole form. However it is useful to have the same parametrization in comparing with the previous experiments, NEUT still uses the same parametrization in the standard configuration. As for the axial-vector coupling constant (axial-vector mass), the value is set to 1.2 GeV/c^2 by default to have good agreements with the recent neutrino experiments [4,5]. The calculated cross-sections compared with the data are shown in Fig. 1 (a) and (b). In each figure, the solid lines correspond to the free target and the dashed lines correspond to the bound target, respectively.

In estimating the cross-sections of neutral current elastic scattering, we use the following relations [12]:

$$\sigma(\nu p \rightarrow \nu p) \;=\; 0.153 \times \sigma(\nu n \rightarrow e^- p)\,,$$

$$\begin{aligned}
\sigma(\bar{\nu}p \to \bar{\nu}p) &= 0.218 \times \sigma\left(\bar{\nu}p \to e^{+}n\right)\,, \\
\sigma(\nu n \to \nu n) &= 1.5 \times \sigma(\nu p \to \nu p)\,, \\
\sigma(\bar{\nu}n \to \bar{\nu}n) &= 1.0 \times \sigma(\bar{\nu}p \to \bar{\nu}p)\,.
\end{aligned}$$

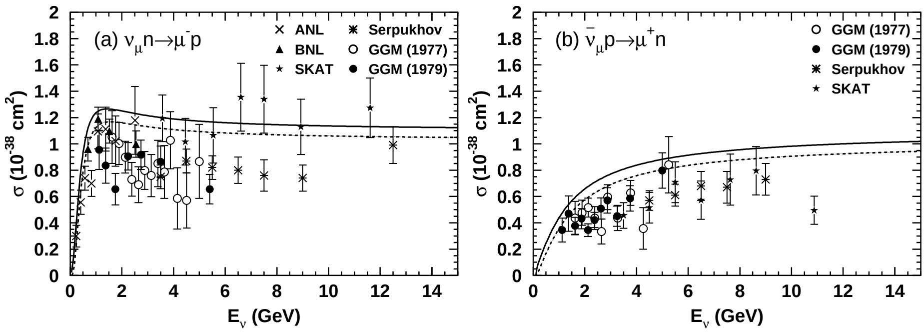

Fig. 1. Cross-sections of charged current quasi-elastic scattering. The solid lines show the calculated cross-sections for free targets and the dashed lines show the calculated cross-section for the bound targets, respectively. The dashed line shows the calculated cross-section of proton in oxygen. Data points are taken from the following experiments: ANL [6], Gargamelle [7, 8], BNL [9], Serpukhov [10] and SKAT [11].

2.2. Single pion, photon, kaon and eta productions

We adopt Rein and Sehgal's method to simulate the neutrino induced single pion productions [13]. In their method, this type of interaction is split into two steps as follows:

$$\nu + N \to l + N^*\,, \qquad N^* \to \pi + N'\,,$$

where N and N' are the nucleons, N^* is the baryon resonances. To obtain the cross-sections, we calculate the amplitudes of each resonance production multiplied by the decay probability of resonance into one pion and one nucleon. At this time, interferences among the resonances are also taken into account. In calculating the cross-sections for these interactions, 18 resonances below 2 GeV/c^2 are considered. For this calculation, the axial-vector mass is set to 1.2 GeV/c^2 by default. In order to avoid double counting of the same interactions in obtaining the total cross-section, the hadronic invariant mass (W), which is the mass of the intermediate resonance, is restricted to be less than 2 GeV/c^2. The calculated cross-sections of the single pion productions and the experimental results are shown in Fig. 2.

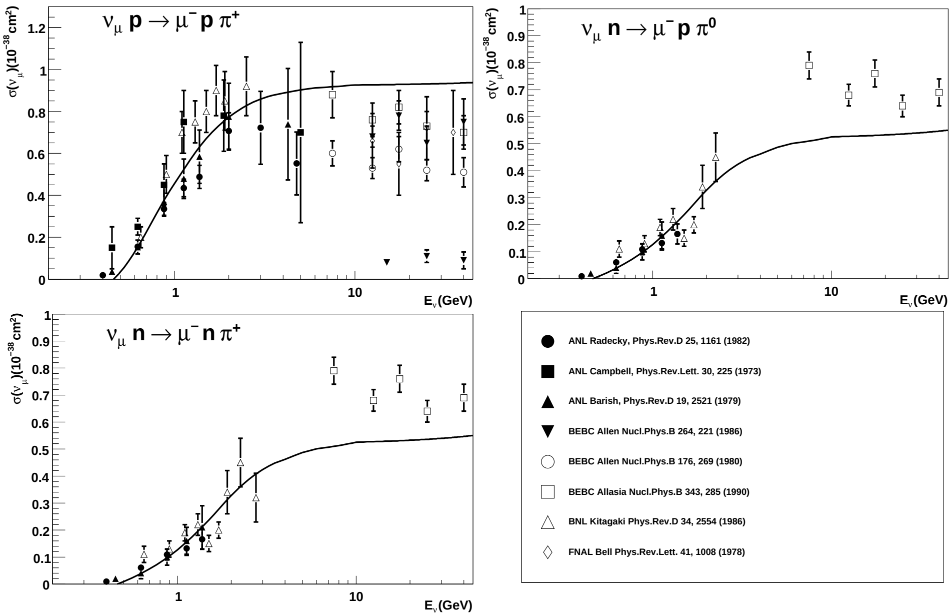

Fig. 2. Cross-sections of (a) $\nu_\mu p \to \mu^- p\pi^+$, (b) $\nu_\mu n \to \mu^- p\pi^0$, (c) $\nu_\mu n \to \mu^- n\pi^+$. Solid lines show the calculated cross-sections. Experimental data points are summarized in the table.

In the determination of the angular distribution of pion in the final state, we use Rein and Sehgal's method for the $P_{33}(1232)$ resonance. For the other resonances, directional distribution of generated pion is set to be isotropic in the Adler Frame (resonance rest frame). With the Rein and Sehgal's model, it is possible to calculate the cross-sections for each individual resonance if we ignore the interferences. Using this characteristics, we made the probability functions to determine whether the intermediate resonance is P_{33} or not with the single-resonance cross-sections. The angular distribution of π^+ has been measured for $\nu p \to \mu^- p\pi^+$ mode [14] and the prediction from the simulation agrees well with the data. We also consider the Pauli blocking effect in the decay of resonances by requiring that the momentum of nucleon should be larger than the Fermi surface momentum. This suppresses the interaction cross-section by a few percent. The pion-less delta decay is also considered and 20% of the events do not have a pion and only the lepton and the nucleon are generated.

As described, the Rein and Sehgal's model provide us the amplitudes of neutrino resonance productions. Therefore, it is also possible to calculate the cross-sections of single photon, K and Eta productions by changing the decay probabilities of the resonances. We also included these interactions in the simulation program.

2.3. Deep inelastic scattering

The cross-section of deep inelastic scattering is calculated by integrating Eq. 1 in the range of $W > 1.3$ GeV/c^2, here W is the invariant mass of the hadronic system:

$$
\begin{aligned}
\frac{d^2\sigma}{dxdy} &= \frac{G_{\mathrm{F}}^2 M_N E_\nu}{\pi}\Big(\left(1 - y + \tfrac{1}{2}y^2 + C_1\right) F_2\left(x, q^2\right) \\
&\quad \pm y\left(1 - \tfrac{1}{2}y + C_2\right)\left[xF_3\left(x, q^2\right)\right] \Big), \\
C_1 &= \frac{yM_l^2}{4M_N E_\nu x} - \frac{xyM_N}{2E_\nu} - \frac{M_l^2}{4E_\nu^2} - \frac{M_l^2}{2M_N E_\nu x}, \\
C_2 &= -\frac{M_l^2}{4M_N E_\nu x},
\end{aligned} \tag{1}
$$

where $x = -q^2/(2M(E_\nu - E_l))$, $y = (E_\nu - E_l)/E_\nu$, M_N is the mass of nucleon, M_l is the mass of lepton, E_ν and E_l are the energy of incoming neutrino and outgoing lepton in the laboratory frame, respectively. The nucleon structure functions, F_2 and xF_3, are taken from the parton distribution function GRV98 [15] with corrections proposed by Bodek and Yang [16] to improve the agreement with the experiments in the low q^2 region. In the actual calculation to obtain the cross-section, we use the probability function of pion multiplicity, which is a function of W and gives the probability to generate more than 1 pion, in the small W region ($W \leq 2$ GeV/c^2). Because the single pion productions are already included in the simulation program and thus, we used this method to obtain the cross-sections of deep inelastic scattering to avoid double counting. The mean multiplicity of charged pions is estimated from the result of the Fermilab 15-foot hydrogen bubble chamber experiment [17] as $\langle n_\pi \rangle = 0.09 + 1.83 \ln W^2$. Total charged current cross-sections including quasi-elastic scattering, single meson productions and deep inelastic scattering are shown in Fig. 3 (a) and (b).

In order to obtain the cross-sections for multi pion production induced by the neutral current, we use the following relations:

$$
\begin{aligned}
\frac{\sigma(\nu N \to \nu X)}{\sigma(\nu N \to \mu^- X)} &= 0.26 \ (E_\nu \leq 3 \text{ GeV}), \\
\frac{\sigma(\nu N \to \nu X)}{\sigma(\nu N \to \mu^- X)} &= 0.26 + 0.04 \times ((E_\nu - 3.)/3.) \\
&\quad (3 \text{ GeV} < E_\nu < 6 \text{ GeV}), \\
\frac{\sigma(\nu N \to \nu X)}{\sigma(\nu N \to \mu^- X)} &= 0.30 \ (E_\nu \geq 6 \text{ GeV}), \\
\frac{\sigma(\bar{\nu} N \to \bar{\nu} X)}{\sigma(\bar{\nu} N \to \mu^+ X)} &= 0.39 \ (E_\nu \leq 3 \text{ GeV}),
\end{aligned}
$$

$$\frac{\sigma(\bar{\nu}N \to \bar{\nu}X)}{\sigma(\bar{\nu}N \to \mu^+X)} = 0.39 - 0.02 \times ((E_\nu - 3.)/3.)$$

$$(3 \text{ GeV} < E_\nu < 6 \text{ GeV}),$$

$$\frac{\sigma(\bar{\nu}N \to \bar{\nu}X)}{\sigma(\bar{\nu}N \to \mu^+X)} = 0.37 \ (E_\nu \geq 6 \text{ GeV}).$$

These values are estimated from the experimental results [29, 30].

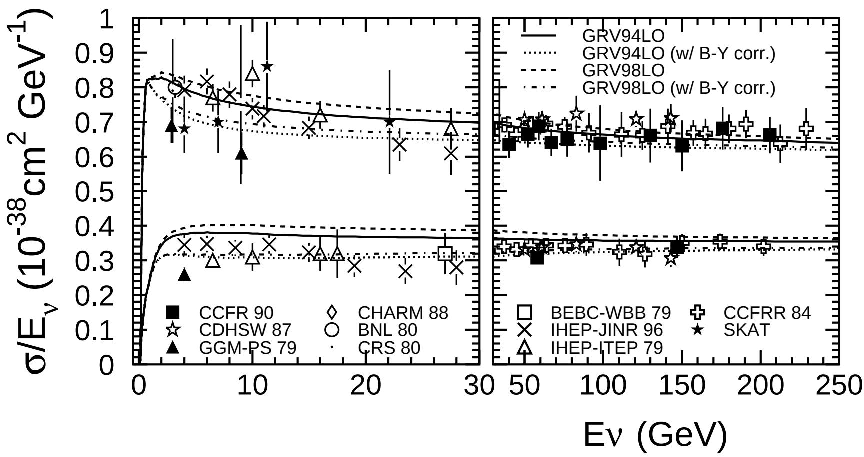

Fig. 3. Neutrino and anti-neutrino charged current total cross-section. The upper 4 lines corresponds to neutrino and lower 4 lines corresponds to the anti neutrino. The meanings of each lines and corresponding data points are shown in the figure. (CCFR90 [18], CDHSW87 [19], GGMPS79 [20], CHARM88 [21], BNL80 [22], CRS80 [23], BEBCWBB79 [24], IHEPJINR96 [25], IHEPITEP79 [26], CCFRR84 [27], SKAT [28]).

In NEUT, both PYTHIA/JetSet and our own codes are used to generate the deep inelastic scattering events because PYTHIA/JetSet was developed to simulate higher energy interactions and does not fit for the lower energies. Therefore, we use the experimental results to generate an event whose W is less than 2 GeV/c^2. For those small W events, we assume KNO scaling to determine the value of W [31]. The multiplicity of pions is determined by the function described before, which was also obtained experimentally. The forward–backward asymmetry of pion multiplicity($n_\pi^{\mathrm{F}}/n_\pi^{\mathrm{B}}$) in the hadronic center of mass system is included as follows:

$$\frac{n_\pi^{\mathrm{F}}}{n_\pi^{\mathrm{B}}} = \frac{0.35 + 0.41 \ln\left(W^2\right)}{0.5 + 0.09 \ln\left(W^2\right)}. \tag{2}$$

This value was obtained from the result of the BEBC experiment [32].

In determining the generated position of the hadrons in nucleus, the concept of the formation length is employed. Based on this idea, hadronization process is not instant and takes some time before generating the hadrons. Therefore, the generated position of hadrons are slightly different from the initial position of neutrino interaction and the formation length (L) is defined as the distance between those two positions. The actual form of L is defined as $L = p/\mu^2$, where p is the momentum of the hadron and μ^2 is the constant parameter determined experimentally. In NEUT, μ^2 is set to 0.08 GeV^2 according to the result from the SKAT experiment [33].

2.4. Coherent pion production

The differential cross-section of neutral current coherent pion production is expressed as follows [34]:

$$\begin{aligned}
\frac{d^3\sigma}{dQ^2 dy dt} &= \frac{G^2 M_N}{2\pi^2} f_\pi^2 A^2 E_\nu (1-y) \frac{1}{16\pi} \left[\sigma_{\mathrm{tot}}^{\pi N}\right]^2 \\
&\quad \times (1+r^2) \left(\frac{m_A^2}{m_A^2 + Q^2}\right)^2 e^{-b|t|} F_{\mathrm{abs}} \,, \\
r &= \mathrm{Re} f_{\pi N}(0) / \mathrm{Im} f_{\pi N}(0) \,,
\end{aligned}$$

where Q^2 is the square of the 4-momentum transfer of lepton, t is the square of the 4-momentum transferred to the nucleus, m_A is the axial-vector mass, $f_\pi = 0.93 m_\pi$, $b = 80$ GeV^{-2}, G is the weak coupling constant, M_N is the mass of nucleon, $y(= (E_\nu - E_l)/E_\nu)$ is the fraction of the lepton's energy loss, E_ν and E_l are the energy of neutrino and outgoing lepton, and A is the atomic number of the target nucleus, respectively. F_{abs}, which accounts for the absorption of pion in the nucleus, is expressed as follows:

$$\begin{aligned}
F_{\mathrm{abs}} &= e^{-\langle x \rangle / \lambda} \,, \\
\lambda^{-1} &= \sigma_{\mathrm{inel}}^{\pi N} \rho \,,
\end{aligned} \tag{3}$$

where $\langle x \rangle$ is the mean path length of the pion in oxygen. $\rho = (\frac{4\pi}{3} R^3)^{-1}$ is the nuclear density, where R is the radius. $\sigma_{\mathrm{tot}}^{\pi N}$ and $\sigma_{\mathrm{tot}}^{\pi N}$ are the averaged total and inelastic pion–nucleon cross-sections, which were obtained from the experimental results and the fitted results are given in the Rein and Sehgal's paper. In order to calculate the charged current cross-section, it is necessary to take into account the effect of lepton mass. The correction factor of the lepton mass (COR) is defined as follows [35]:

$$\mathrm{COR} = 2\left(1 - \frac{1}{2}\frac{Q^2_{\mathrm{min}}}{Q^2 + m_\pi^2}\right)^2 + \frac{1}{4} y \frac{Q^2_{\mathrm{min}}\left(Q^2 - Q^2_{\mathrm{min}}\right)}{(Q^2 + m_\pi^2)^2} \,, \tag{4}$$

$$Q^2_{\mathrm{min}} = m_l^2 \frac{y}{1-y} \,. \tag{5}$$

The obtained cross-section of coherent pion productions are shown in Fig. 4 together with the experimental data points.

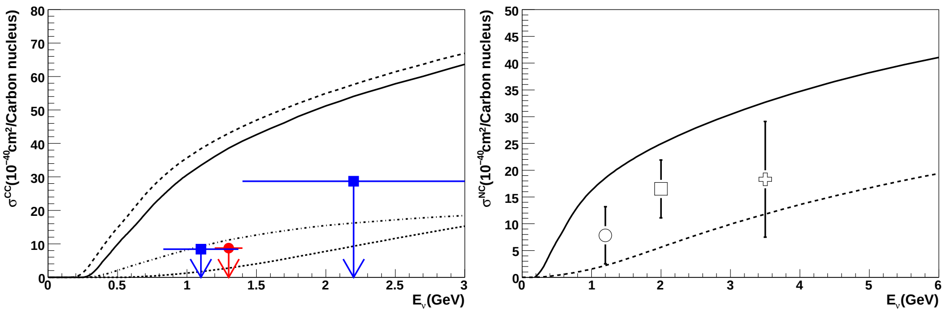

Fig. 4. The cross-sections of coherent pion production off carbon nucleus. Figure left and right correspond to the charged and neutral current, respectively. The solid line shows the cross-section using the model by Rein and Sehgal [35]. The dotted and dash-dotted curve correspond to the model of Kartavtsev *et al.* [36] and Alvarez-Russo *et al.* [37], respectively. The filled boxes and filled circle show the upper limit from the measurement by the K2K [38] and the SciBooNE [39] experiments, respectively. The open circle, open box and open cross correspond to the result from the MiniBooNE [40], Aachen–Padova [41] and Gargamelle [42] experiments, respectively.

3. Nuclear effects

3.1. Introduction

In order to identify the neutrino interaction, experiments use the observed particles in the detector. However, hadrons generated by the neutrino interactions in nucleus are known to interact within the nucleus. As a result, the observed particles in the detector are not always the same as the ones generated by the primary neutrino interaction. Therefore, the interactions of pions, kaons, etas and nucleons in the target nucleus are also simulated in NEUT. All these interactions are treated by using the cascade model but implementations are slightly different for different kinds of hadrons. Basic procedure of the simulation is as follows. First, move the particle by unit length starting from the generated point of hadrons. Then, determine whether one of the interactions has happened or not based on the interaction probability. If no interactions happened in this step, move the particle again. This procedure is repeated until there is an interaction occurring to the particle or the particle exits from the nucleus. The starting point of the hadron is defined to be the same as the interaction point of the neutrino except for the deep inelastic scattering. The interaction position of the neutrino in nucleus is selected by using the Woods–Saxon type nucleon density distribution. If the primary interaction was deep inelastic scattering, hadronization point is shifted using the idea of formation length as already described.

3.2. Pion interactions in nucleus

The neutrino pion production is one of the dominant interactions in a few-GeV region and the interaction cross-sections of pions in nucleus from those interactions are quite large. Because the large fraction of pions are originated from the resonances and this implies that the resulting pions have large cross-section with nucleon. Therefore, the interactions of pions in nucleus have large effects in the various studies using the water Cherenkov detector.

In NEUT, following pion interactions in nucleus are considered: inelastic scattering, charge exchange and absorption. Also, particle production is taken into account for the high energy pions. The interaction probabilities for the pion, whose momentum is smaller than 500 MeV/c, are calculated following the method of Oset *et al.* [43]. In their model, Fermi motion of the nucleon in the nucleus and the Pauli blocking effect were taken into account. Here, the Fermi surface momentum ($p_{\mathrm{F}}(r)$) in the nucleus shows dependence on the density (local density approximation) and is defined as follows: $p_{\mathrm{F}}(\boldsymbol{r}) = [\frac{3}{2}\pi^2\rho|\boldsymbol{r}|]^{-\frac{1}{3}}$, where $\rho(\boldsymbol{r}) = \frac{Z}{A}\bar{\rho}\{1+\exp(\frac{|\boldsymbol{r}|-c}{a})\}^{-1}$, here A is the mass number, Z is the atomic number, $\bar{\rho}$ is the average density of nucleus, a and c are the density parameters of nucleus, respectively. As a result, the calculated interaction probabilities show dependence on both the momentum of pion and the position of pion in the nucleus. The direction and momentum of pion after the interaction are determined by using the results of phase shift analysis obtained from the π–N scattering experiments [44] with medium correction suggested by Seki *et al.* [45]. Again, the Pauli blocking effect is also taken into account by requiring the nucleon momentum after interaction to be larger than the Fermi surface momentum, when calculating the pion scattering amplitude.

The interaction probabilities of pion, whose momentum is higher than 500 MeV/c, are extracted from the experimental data of the π–N scattering experiments. For this case, these interaction probabilities depend only on the momentum of the pion.

This pion interaction simulation is tested by using the following three interactions: π^{12}C scattering, π^{16}O scattering and pion photo-production ($\gamma+^{12}\mathrm{C} \to \pi^- + X$). One of the comparisons with the existing experimental data is shown in Fig. 5.

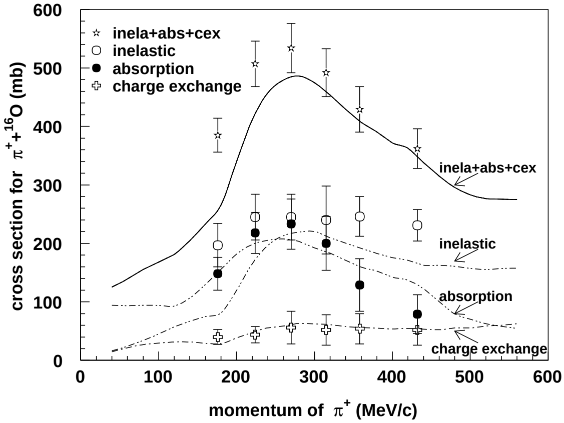

Fig. 5. Interaction cross-sections of $\pi^+ + {}^{12}C$ scattering as a function of momentum of the incident π^+. The three lines shows the result of Monte Carlo simulation. Data points are taken from Ref. [46]. The solid line and circles correspond to the inelastic scattering, the dashed line and squares correspond to the absorption and the dotted line and triangles correspond to the charge exchange interaction, respectively.

The resulting interaction probabilities of π^+ in oxygen are shown in Fig. 6.

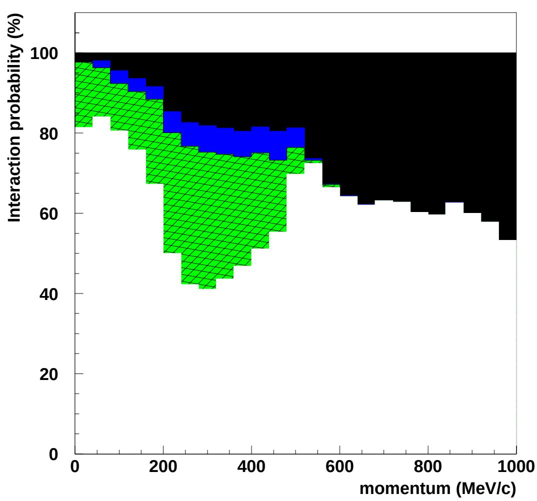

Fig. 6. Interaction probabilities of π^+ in ${}^{16}O$. The filled area corresponds to the inelastic scattering including particle production, the shaded area corresponds to the charge exchange interaction, the hatched area corresponds to the absorption, and blank area corresponds to the escaped pions without interaction, respectively.

3.3. Kaon and eta interactions in nucleus

The interactions of kaons in oxygen is also considered by using the similar method to simulate pion interactions. The differential cross-sections and determination of the kinematics are done by using the results of KN and $\bar{K}N$ scattering experiments [47].

The absorption of η ($\eta N \to N^* \to \pi(\pi)N$) is also considered [48]. Because the efficiency and background estimation of nucleon decay into η will be affected by this process. The relevant nucleon resonances are N(1540) and N(1650) and the cross-section for $\eta N \to \pi(\pi)N$ is calculated by using the following formula:

$$\sigma = \frac{\pi}{k^2}\left(J + \frac{1}{2}\right)\frac{\Gamma_{\eta N}\Gamma_{\pi(\pi)N}}{(W - M^*)^2 + \Gamma_{\mathrm{tot}}/4}, \tag{6}$$

where k is the momentum of η in the center of mass system, J is the spin of the resonance, Γ is the width of the resonance, W is the invariant mass of the ηN system and M^* is the mass of the resonance, respectively. The pions from this process are also tracked as described before.

3.4. Nucleon interactions in nucleus

The nucleon rescattering in the nucleus affects the identification of the neutrino interaction mode because the quasi-elastic scattering is identified by using the direction of muon and the knock out nucleon in the tracking detectors. Therefore, the understanding of the nucleon interactions is also important.

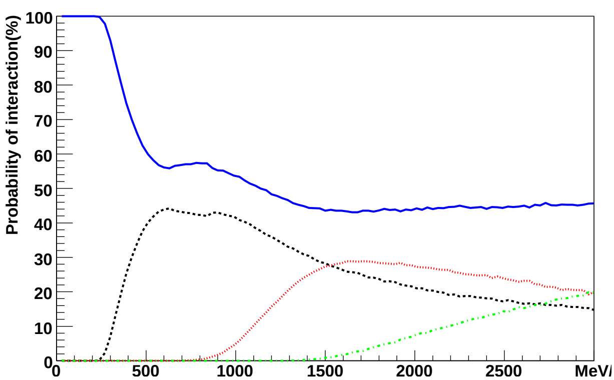

Fig. 7. Interaction probabilities of nucleon in ^{16}O as a function of nucleon momentum. The solid curve, the dashed curve, the dotted curve and the dash-dotted curve correspond to no interaction, elastic scattering, single pion production and double pion production, respectively.

In order to simulate the nucleon rescattering, almost the same cascade model as used for the pion simulation has been implemented. The considered interactions are elastic scattering, a single or two delta(s) production for the pion production. The interaction probabilities are extracted from the existing data of differential cross-sections from nucleon–nucleon scattering experiments [49], which are also used in GCALOR. The delta productions are simulated based on the isobar production model by Lindenbaum *et al.* [50]. The resulting interaction probabilities of nucleon in ^{16}O is shown in Fig. 7.

The author would like to thank the Collaborations of Kamiokande, Super-Kamiokande, K2K, SciBooNE and T2K. NEUT has been developed and updated by the collaboration works of these experiments.

REFERENCES

[1] M. Nakahata *et al.*, *J. Phys. Soc. Jpn.* **55**, 3786 (1986).
[2] C.H. Llewellyn-Smith, *Phys. Rep.* **C3**, 261 (1972).
[3] R.A. Smith, E.J. Moniz, *Nucl. Phys.* **B43**, 605 (1972); **B101**, 547(E) (1975).
[4] M.H. Ahn *et al.*, *Phys. Rev.* **D74**, 072003 (2006).
[5] A.A. Aguilar-Arevalo *et al.*, *Phys. Rev. Lett.* **100**, 032301 (2008).
[6] S. Barish *et al.*, *Phys. Rev.* **D16**, 3103 (1977).
[7] S. Bonetti *et al.*, *Nouvo Cim.* **38**, 260 (1977).
[8] M. Pohl *et al.*, *Nuovo Cim.* **26**, 332 (1979); N. Arimenise *et al.*, *Nucl. Phys.* **B152**, 365 (1979).
[9] A.S. Vovenko *et al.*, *Yad. Fiz.* **30**, 1014 (1979).
[10] S. Belikov *et al.*, *Z. Phys.* **320**, 625 (1985).
[11] J. Brunner *et al.*, *Z. Phys.* **C45**, 551 (1990).
[12] K. Abe *et al.*, *Phys. Rev. Lett.* **56**, 1107 (1986); C.H. Albright *et al.*, *Phys. Rev.* **D14**, 1780 (1976).
[13] D. Rein, L.M. Sehgal, *Ann. Phys.* **133**, 79 (1981); D. Rein, *Z. Phys.* **C35**, 43 (1987).
[14] T. Kitagaki *et al.*, *Phys. Rev.* **D34**, 2554 (1986).
[15] M. Glück, E. Reya, A. Vogt, *Eur. Phys. J.* **C5**, 461 (1998).
[16] A. Bodek, U.K. Yang, `hep-ex/0308007`.
[17] S.J. Barish *et al.*, *Phys. Rev.* **D17**, 1 (1978).
[18] P.S. Auchincloss *et al.*, *Z. Phys.* **C38**, 411 (1990).
[19] P. Berge *et al.*, *Z. Phys.* **C35**, 443 (1987).
[20] S. Campolillo *et al.*, *Phys. Lett.* **84B**, 281 (1979).
[21] J.V. Allaby *et al.* [CHARM Collaboration], *Z. Phys.* **C38**, 403 (1988).

[22] N.J. Bker *et al.*, *Phys. Rev.* **D25**, 617 (1972).
[23] C. Baltay *et al.*, *Phys. Rev. Lett.* **44**, 916 (1980).
[24] D.C. Colley *et al.*, *Z. Phys.* **C2**, 197 (1979).
[25] V.B. Anikeev *et al.*, *Z. Phys.* **C70**, 39 (1996).
[26] A.S. Vovenko *et al.*, *Sov. J. Nucl. Phys.* **30**, 527 (1979).
[27] D.B. MacFarlane *et al.*, *Z. Phys.* **C26**, 1 (1984).
[28] D.S. Baranov *et al.*, *Phys. Lett.* **B81**, 255 (1979).
[29] P. Musset, J.-P. Vialle, *Phys. Rep.* **C39**, 1 (1978).
[30] J.E. Kim *et al.*, *Rev. Mod. Phys.* **53**, 211 (1981).
[31] H. Sarikko, *Neutrino*, 507 (1979).
[32] S. Barlag *et al. Z. Phys.* **C11**, 283 (1982).
[33] V. Ammosov, talk at NuInt01 workshop at KEK, Tsukuba, Japan 2001.
[34] D. Rein, L.M. Sehgal, *Nucl. Phys.* **B223**, 29 (1983); P. Marage *et al.*, *Z. Phys.* **C31**, 191 (1986).
[35] D. Rein, L.M. Sehgal, *Phys. Lett.* **B657**, 207 (2007).
[36] A. Kartavtsev, E.A. Paschos, G.J. Gounaris, *Phys. Rev.* **D74**, 054007 (2006).
[37] L. Alvarez-Ruso *et al.*, *Phys. Rev.* **C75**, 055501 (2007).
[38] M. Hasegawa *et al.*, *Phys. Rev. Lett.* **95**, 252301 (2005).
[39] K. Hiraide *et al.*, *Phys. Rev.* **D78**, 112004 (2008).
[40] J.L. Raaf, Ph.D. thesis, University of Cincinnati, 2005.
[41] H. Faissner *et al.*, *Phys. Lett.* **B125**, 230 (1983).
[42] E. Isiksal, D. Rein, J.G. Morfin, *Phys. Rev. Lett.* **52**, 1096 (1984).
[43] L.L. Salcedo *et al.*, *Nucl. Phys.* **A484**, 557 (1988); private communication with H. Toki.
[44] G. Rowe *et al.*, *Phys. Rev.* **C18**, 584 (1978).
[45] R. Seki, K. Masutani, *Phys. Rev.* **C27**, 2799 (1983).
[46] D. Ashery *et al.*, *Phys. Rev.* **C23**, 2173 (1981).
[47] B.R. Martin, M.K. Pidcock, *Nucl. Phys.* **B126**, 266 (1977); **B126**, 285 (1977); J.S. Hyslop *et al.*, *Phys. Rev.* **D46**, 961 (1992).
[48] D.A. Sparrow, Proc. of the Conf. on the Intersection Between Particle and Nuclear Physics, 1019 (1984).
[49] H.W. Bertini, *Phys. Rev.* **C6**, 631 (1972).
[50] S.J. Lindenbaum *et al.*, *Phys. Rev.* **105**, 1874 (1957).